

Supplementary Information:

Section 1: Convective Effect on macroelectrode with different orientations

This section presents if and how the density driven natural convective flows influence the voltammetric response when the electrode changes its orientation. The chronoamperometric response was obtained by applying a constant potential of 0.35 V for 60 s for the oxidation of 1 mM ferrocene methanol at 25 °C. The results show that the convection is negligible when the electrode is horizontal facing downwards or upwards within experimental reproducibility while about 10% extra currents ($(I_{\text{exp}} - I_{\text{Shoup-Szabo}})/I_{\text{Shoup-Szabo}}$) were obtained due to the natural convection on a vertical macroelectrode, where i_{exp} is the experimental measured current and $i_{\text{Shoup-Szabo}}$ is the predicted current which accounts for both linear and radial diffusional currents on the basis of Shoup-Szabo equation¹. The detail of the cell design and the results for vertical electrodes are shown below.

The Shoup Szabo equation¹ is given by:

$$\frac{I(t)}{n\pi FcDr} = 1 + \frac{r}{\sqrt{\pi Dt}} + \left(\frac{4}{\pi} - 1\right) \exp\left(\frac{r^2}{4Dt}\right) \exp\left(-\frac{0.39115r}{\sqrt{Dt}}\right)$$

where n is the number of electrons transferred, F is the Faraday constant, c is the bulk concentration of the reactant, D is the diffusion coefficient of the reactant, r is the radius of the electrode, t is the time. In the present case of ferrocene methanol a diffusion coefficient of $7.8 \times 10^{-10} \text{ m}^2 \text{ s}^{-1}$ was chosen in the calculation.²

Section 1.1 Electrochemical cell design

This section presents the schematic of working electrode (Figure 1(a)) and the cell design (Figure 1(b)) including the geometry and position of working electrode. A screen printed platinum macroelectrode (SPPE) was used as the working electrode. Its own reference and counter electrodes were covered using insulating tape. The Pt working electrode left was connected to a metal wire using silver epoxy. The saturated calomel electrode and silver wire were used as reference electrode and counter electrode, respectively.

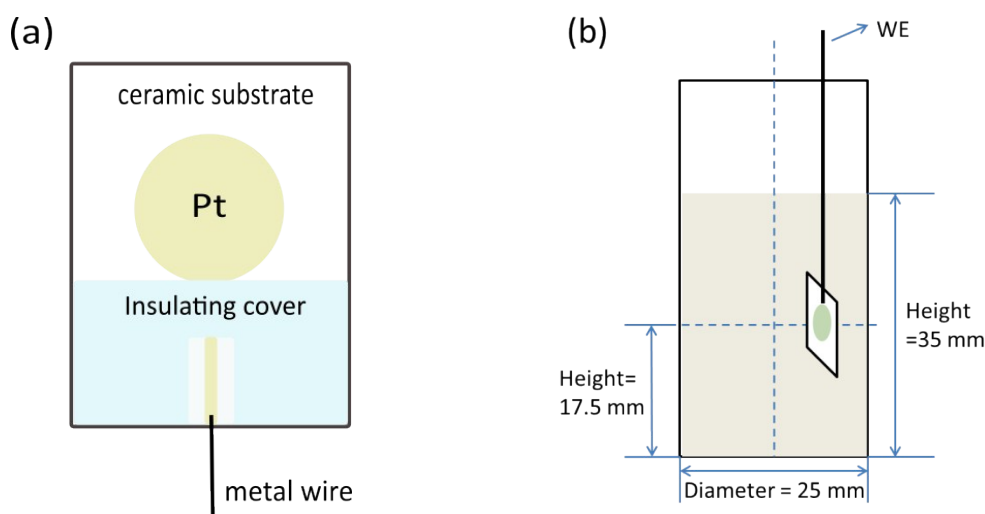


Figure 1 Schematic of vertical SPPE (a) and the cell design (b). WE represents for working electrode (SPPE).

Section 1.2: Vertical electrode

Figure 2 below presents the experimental (red) recorded chronoamperometric response for the oxidation of 1 mM ferrocene methanol at 25°C at a vertical SPPE plotted against the predicted (brown) response on the basis of Shoup-Szabo equation. The inlay shows the normalised difference ($i_{\text{exp}} - i_{\text{Shoup-Szabo}} / i_{\text{Shoup-Szabo}}$) of chronoamperometric response. The result shows that at long time scale (> 20 s), the current becomes larger compared to the predicted current, proving the existence of density driven convective flow. At 60 s, around 10% extra current was contributed from natural convection.

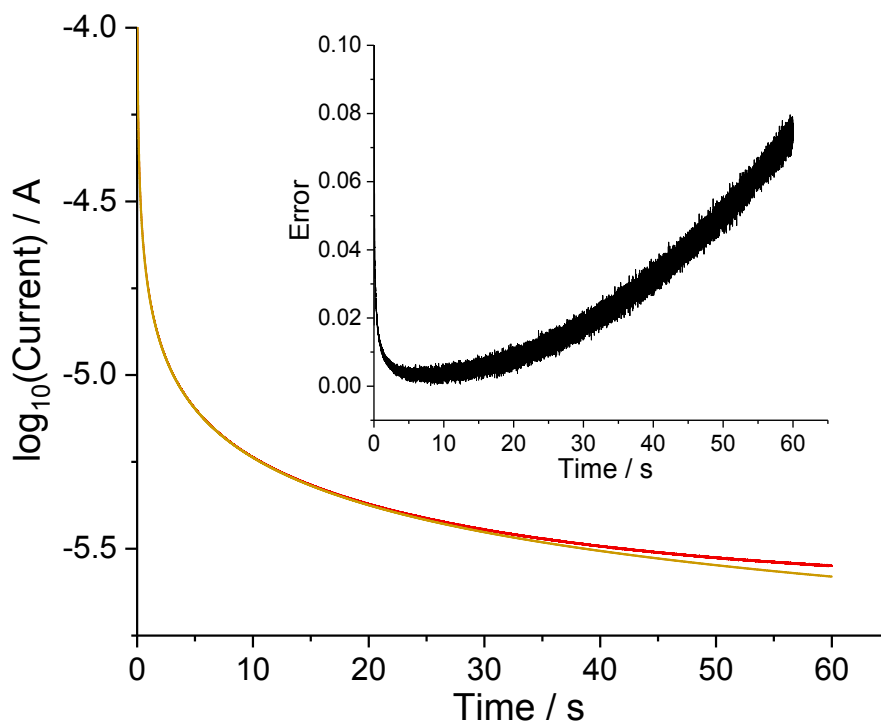


Figure 2 The experimentally recorded chronoamperometric response of a vertical SPPE (red) ($r = 0.185$ cm) plotted against that predicted on the basis of Shoup-Szabo equations (brown). Inlay in (a) depicts the error between the experimental (red) and simulated chronoamperometric response that predicted by the Shoup-Szabo equation (brown).

Section 2:

The Shoup Szabo equation¹ is given by:

$$\frac{I(t)}{n\pi FcDr} = 1 + \frac{r}{\sqrt{\pi Dt}} + \left(\frac{4}{\pi} - 1\right) \exp\left(\frac{-0.39115r}{\sqrt{Dt}}\right)$$

In the present case of ferrocene methanol a diffusion coefficient of $7.8 \times 10^{-10} \text{ m}^2 \text{ s}^{-1}$ was chosen in the simulation.²

It should be noted that the Shoup-Szabo equation¹ is itself approximate being based on fitting to simulations and can be in error by up to 0.6%. Consequently the inlay of Figure 3 a) of the main text marginally over-estimates the discrepancy between the experimental and theoretically predicted results.

Figure 3 below presents the plot of the normalised difference ($i_{\text{exp}} - i_{\text{sim}} / i_{\text{sim}}$) of chronoamperometric response for the oxidation of 1 mM ferrocene methanol at 25°C at a glassy carbon macroelectrode, where i_{exp} is the experimental measured current and i_{sim} is the simulated current response. The simulation was based on a two-dimensional microdisc model solved using the ADI method.³ This result shows that with the consideration of radial diffusion, the response on a macroelectrode can be predicted with an average error of 1.1%.

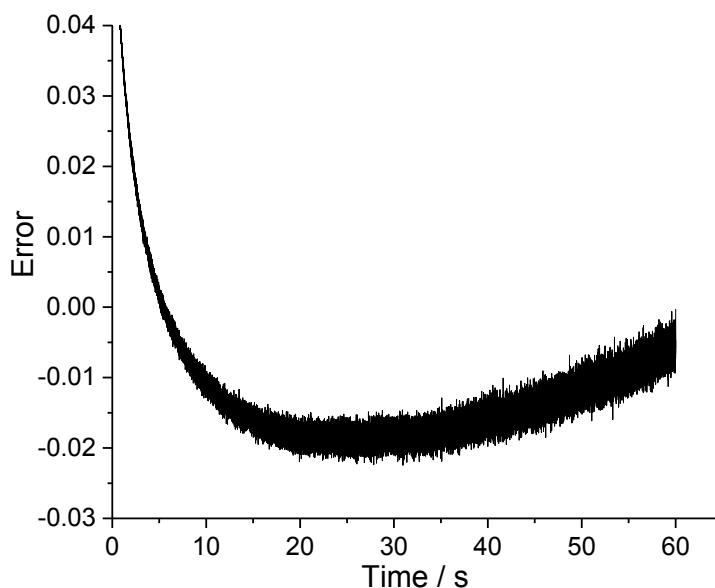


Figure 3 Error between the experimental and simulated chronoamperometric response in 1 mM ferrocene methanol solution on a glassy carbon macroelectrode (3 mm in diameter). The error = $[i_{\text{(exp)}} - i_{\text{(sim)}}] / i_{\text{(sim)}}$.

Section 3: Evidence for evaporation effect on voltammetric behaviour

Figure 4 presents the experimental voltammograms of a carbon fibre microcylinder electrode in a closed cell as a function of time. It shows that the voltammetric response is reproducible with time and the importance of avoiding evaporative losses.

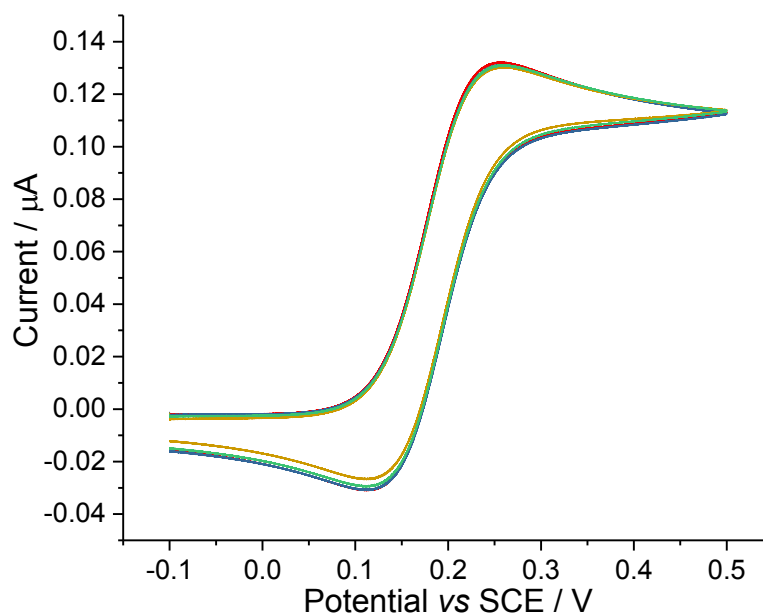


Figure 4 Voltammograms on a carbon fibre microcylinder electrode in a closed cell as a function of time, 0 minutes (red), 15 minutes (blue), 30 minutes (brown) and 45 minutes (green) after the cell has been thermostated and allowed to equilibrate (~ 10 mins) The experiments were run in 1 mM Ferrocene methanol with 0.1 M KCl. Scan rate $\nu = 25 \text{ mV s}^{-1}$; temperature $T = 25^\circ\text{C}$.

Section 4: Evidence for the vibration effect on voltammetric behaviour

This section presents the comparison between a normal water bath thermostat system and optimised thermostated electrochemical cell as used in the main body of the text. Here in the conventional cell system the electrochemical cell is held in place in a thermostated water bath using a laboratory clamp and held by a clamp stand. Figure 5 shows how the voltammetric response varies with time in both cell conditions; the comparison between the experimental and simulated voltammograms is shown in Figure 6. These results show that at short times in the normal electrochemical system the microcylinder electrode exhibits a near steady state response (Figure 5 (a) red line), over time (ca. minutes) the system stabilises towards a more peaked and hence more diffusional response. This behaviour is interpreted on the likely basis of the cell not being held fully rigidly in place despite being ‘clamped’ and as time goes on the vibration of the cell or the effect of vibration decreases minimising the magnitude of the convective contribution to the measured Faradaic current at high overpotentials. It is important to note that in this cell design where a water bath has been used to control the cells temperature the voltammetric response, even at long times, does not become purely diffusional as evidenced through comparison of the voltammetric waveshape with that predicted by numerical simulation as shown in Figure 6 (DigiSim; see experimental section).

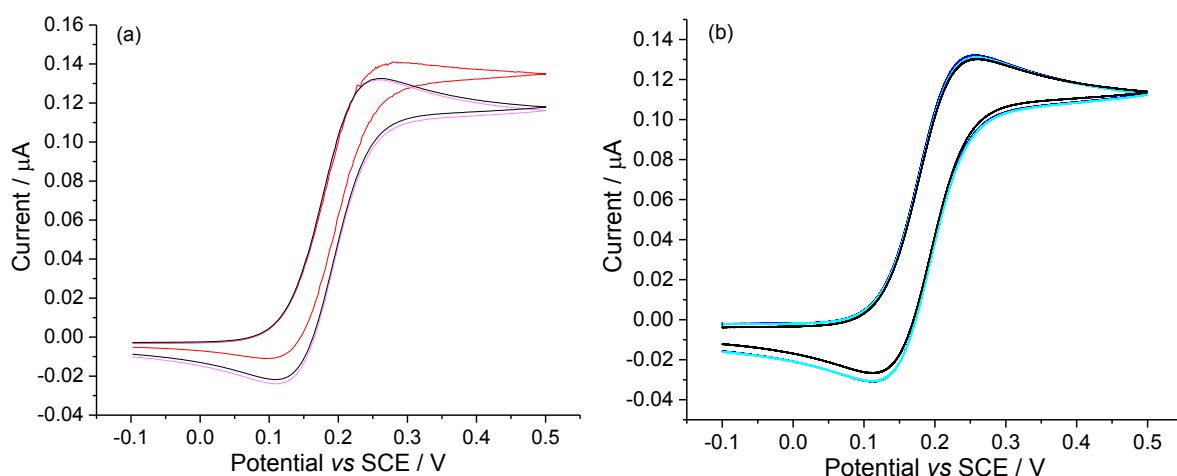


Figure 5 The oxidation of ferrocene methanol (1 mM) at 25°C at a carbon fibre microcylinder electrode ($r=3.5\ \mu\text{m}$, $l=0.916\ \text{mm}$) as a function of time in a closed cell in (a) conventional water bath system (clamp stand) and (b) optimised thermostated electrochemical cell. Scan rate $v=25\ \text{mV s}^{-1}$; temperature $T=25\ ^\circ\text{C}$. In Figure 1(a), the red, magenta and gray curves represent the voltammograms at the time of 0 s, 600 s and 1200 s respectively. In figure 1(b), blue, cyan and black curves represent the voltammograms at the time of 0 s, 600 s and 1200 s respectively.

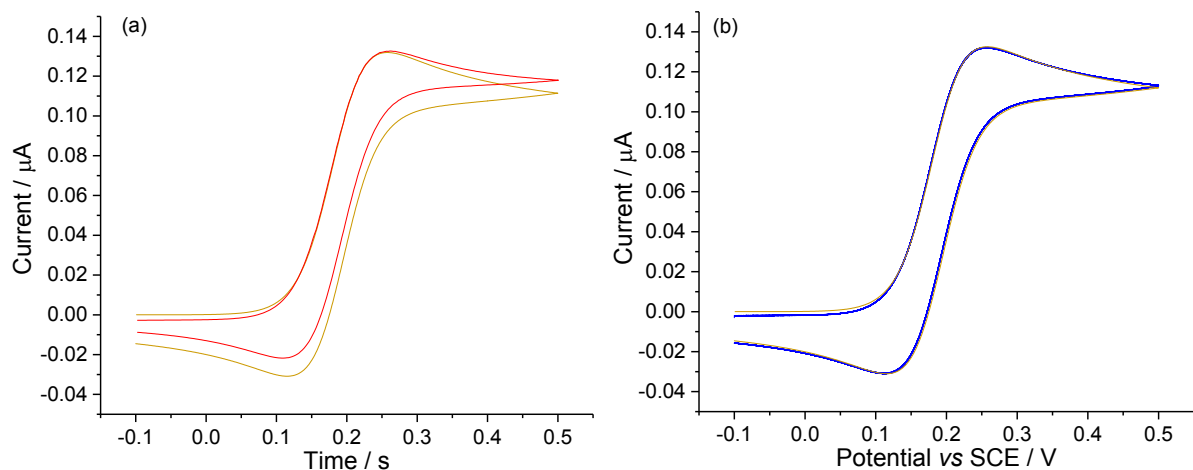


Figure 6 Comparison of experimental (red in (a), blue in (b)) and simulated (yellow) voltammograms for a carbon fibre microcylinder electrode in (a) water bath and (b) optimised thermostated electrochemical cell. The brown curves in both figures were obtained from simulation. Parameters used in the simulation: scan rate $v=25 \text{ mV s}^{-1}$; temperature $T=25 \text{ }^{\circ}\text{C}$; formal potential $E^{\circ}=0.1872 \text{ V}$; electron transfer rate constant $k=10 \text{ m s}^{-1}$; diffusion coefficient $D=7.81 \times 10^{-10} \text{ m}^2 \text{ s}^{-1}$; transfer coefficient $\alpha_a=\alpha_c=0.5$; radius of the electrode $r=3.5 \mu\text{m}$, length of the electrode $l=0.092 \text{ cm}$.

Section 5: Evidence for radial diffusion on macroelectrode

Since in Amatore *et al.*'s paper, an elliptic Pt disk of 1.2 mm equivalent diameter obtained from the slant cross-section (45°) of a 1 mm diameter platinum wire was used.⁴ Here we use a 'elliptic disk' model adapted from Dudko *et al.*'s paper⁵ to predict the chronoamperometric response. These results should be compared to Figure 4 in Amatore's paper⁴, the difference between the theoretical (with radial diffusion) and Cottrellian chronoamperometric responses in Figure 7 (below) shows that the radial diffusion is likely important in their experimental setup and should have been considered. These results indicate that at least 50% of their measured current discrepancy can be understood in terms of the radial diffusion contribution. However, we speculate the remaining 'missing' current may be due to a) evaporative losses causing bulk fluid motion b) electrode vibrations or c) 'spontaneous' convection as defined by Levich i.e. convection arising due to density changes associated with the occurrence of the electrochemical reaction. We note that Amatore *et al.* do discuss the latter point but do not provide evidence that such convection is not operative.

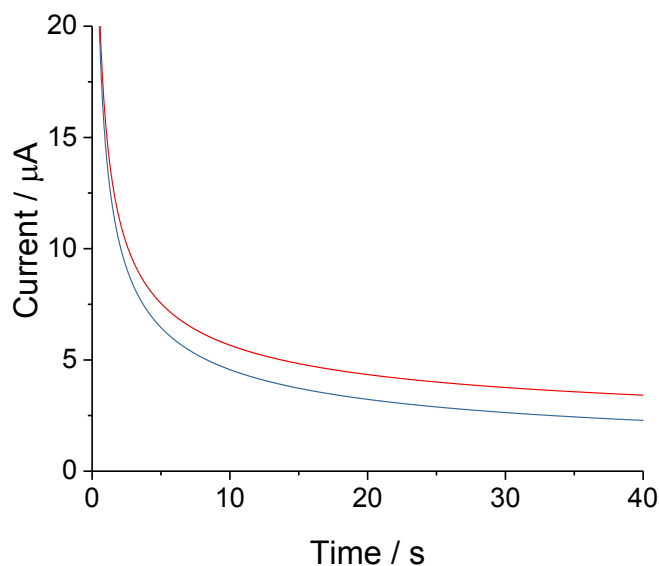


Figure 7 The comparison between the predicted chronoamperometric response from (blue) Cottrell equation and (red) the 'elliptic disk' equation taken from Dudko *et al.*'s paper[3]. All parameters used were the same as those in Amatore *et al.*'s paper: $D(\text{Fe}(\text{CN})_6^{4-}) = (5.7 \pm 0.5) \times 10^{-10} \text{ m}^2 \text{ s}^{-1}$, the concentration $c = 10 \text{ mM}$.

Section 6: Geometry of electrodes

This section shows the description-in-detail of electrodes used. The carbon fibre tip electrode used was imaged using Scanning Electron Microscope (SEM) as shown in Figure 8.

Since the disc electrodes used are both in the macro-scale, it is not possible to show the whole image of the whole electrode surface including the insulating sheath using either optical microscope or SEM. Hence the two disc electrodes are only described as following. For the commercial macrodisc electrode, the diameter of glassy carbon is 2.98 mm and the total diameter of the electrode (i.e. including the insulating sheath) is 6 mm; for the commercial microdisc electrode, the diameter of carbon fibre is 33 μm and the total diameter of the electrode (i.e. including the glass sheath) is 3.5 mm.

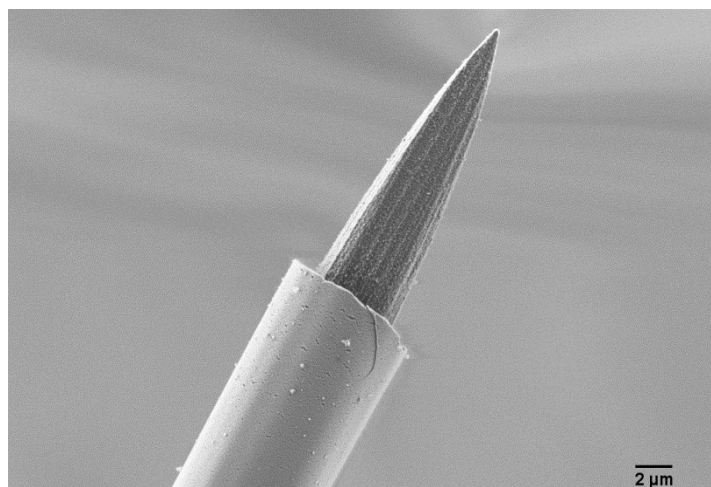


Figure 8 SEM image of a carbon fibre tip electrode.

References:

1. D. Shoup and A. Szabo, *J. Electroanal. Chem. Interfacial Electrochem.*, 1982, **140**, 237-245.
2. K. Ngamchuea, C. Lin, C. Batchelor-McAuley and R. G. Compton, *Anal. Chem.*, 2017, **89**, 3780-3786.
3. R. G. Compton, E. Laborda and K. R. Ward, *Understanding Voltammetry: Simulation Of Electrode Processes*, World Scientific Publishing Company 2013.
4. C. Amatore, S. Szunerits, L. Thouin and J.-S. Warkocz, *J. Electroanal. Chem.*, 2001, **500**, 62-70.
5. O. K. Dudko, A. Szabo, J. Ketter and R. M. Wightman, *J. Electroanal. Chem.*, 2006, **586**, 18-22.